

Electrostatic Environment of Hemes in Proteins:  $pK_a$ s of Hydroxyl Ligands<sup>†</sup>

Yifan Song, Junjun Mao, and M. R. Gunner\*

Physics Department J-419, City College of New York, 138th Street and Convent Avenue, New York, New York 10031

Received October 25, 2005; Revised Manuscript Received April 17, 2006

**ABSTRACT:** The  $pK_a$ s of ferric aquo–heme and aquo–heme electrochemical midpoints ( $E_{ms}$ ) at pH 7 in sperm whale myoglobin, *Aplysia* myoglobin, hemoglobin I, heme oxygenase 1, horseradish peroxidase and cytochrome *c* oxidase were calculated with Multi-Conformation Continuum Electrostatics (MCCE). The  $pK_a$ s span 3.3 pH units from 7.6 in heme oxygenase 1 to 10.9 in peroxidase, and the  $E_{ms}$  range from –250 mV in peroxidase to 125 mV in *Aplysia* myoglobin. Proteins with higher in situ ferric aquo–heme  $pK_a$ s tend to have lower  $E_{ms}$ . Both changes arise from the protein stabilizing a positively charged heme. However, compared with values in solution, the protein shifts the aquo–heme  $E_{ms}$  more than the  $pK_a$ s. Thus, the protein has a larger effective dielectric constant for the protonation reaction, showing that electron and proton transfers are coupled to different conformational changes that are captured in the MCCE analysis. The calculations reveal a breakdown in the classical continuum electrostatic analysis of pairwise interactions. Comparisons with DFT calculations show that Coulomb's law overestimates the large unfavorable interactions between the ferric water–heme and positively charged groups facing the heme plane by as much as 60%. If interactions with Cu<sub>B</sub> in cytochrome *c* oxidase and Arg 38 in horseradish peroxidase are not corrected, the  $pK_a$  calculations are in error by as much as 6 pH units. With DFT corrected interactions calculated  $pK_a$ s and  $E_{ms}$  differ from measured values by less than 1 pH unit or 35 mV, respectively. The in situ aquo–heme  $pK_a$  is important for the function of cytochrome *c* oxidase since it helps to control the stoichiometry of proton uptake coupled to electron transfer [Song, Michonova-Alexova, and Gunner (2006) *Biochemistry* 45, 7959–7975].

Heme cofactors are found in many proteins. Cytochromes having two axial ligands contributed by the protein are six-coordinate and function as redox intermediates in electron transfer chains. However, five-coordinate hemes with one His ligand and one open position are the most common heme motif (1). The open site can bind different molecules for transport or catalysis. Hemoglobins and myoglobins are O<sub>2</sub> transporters (2). Heme oxygenase is an essential protein in heme metabolism, using three O<sub>2</sub>s and seven electrons to degrade heme to biliverdin (3). Peroxidases reduce toxic hydrogen peroxide to water and then carry out one electron oxidization of a wide range of substrates (4, 5). Cytochrome *c* oxidase is the terminal electron acceptor in the respiratory chain (6–9). Here Heme *a*<sub>3</sub> forms a binuclear center with a copper complex (Cu<sub>B</sub>) that reduces O<sub>2</sub> to water. The protein uses the released chemical energy to pump protons across the membrane. Other five-coordinate heme proteins carry out NO storage and transport (10), steroid synthesis (11, 12), and O<sub>2</sub>, CO, and NO sensing (13, 14).

Hemes can carry out many biological functions because the protein, especially the active site residues, modulates the ligand binding specificity and resultant chemistry. The diversity of in situ heme functions highlights important interactions of proteins with their cofactors and substrates. Extensive studies have explored how ligand geometry (15–17) and the protein scaffolding (18) affect in situ heme

properties (1). The range of redox free energy and  $pK_a$ s of protein-bound hemes and their ligands show the importance of electrostatic interactions (19, 20). For example, six-coordinate bis-His–hemes have  $E_{ms}$  ranging from –410 to +360 mV with the redox differences being predominately due to the intraprotein electrostatic environment (1, 20–22). In these proteins the loss of solvation energy (15, 23, 24), interactions with the protein backbone and with other residues (15, 20–22, 25), and local conformation changes on ionization changes (20, 26) determine the thermodynamic equilibrium measured by  $pK_a$ s and  $E_{ms}$ .

Theoretical studies have analyzed hemes in different systems using a number of techniques. The large span of  $E_{ms}$  in cytochromes has been subject to analysis by Protein Dipole Langevin Dipole (PDL) (27, 28), continuum electrostatics (CE)<sup>1</sup> (20, 21, 29, 30), and other techniques (31–37).  $E_{ms}$  of the two hemes in quinol:fumarate reductase have been determined within 30 mV of experimental values using MCCE, allowing the low- and high-potential heme to be assigned to the distal and proximal positions in the structure (38). The heme propionic acid  $pK_a$ s and their influence on the pH dependence of cytochrome  $E_{ms}$  have been considered by CE analysis (20, 38–40). The  $pK_a$ s and

<sup>1</sup> Abbreviations:  $pK_{a,sol}$ , group  $pK_a$  in aqueous solution;  $E_{m,sol}$ , electrochemical midpoint potential ( $E_m$ ) of a model for the redox cofactor in aqueous solution; CE, continuum electrostatics; MCCE, Multi-Conformation Continuum Electrostatics; DFT, density functional theory. 1 ΔpK unit = 1.36 kcal/mol = 58 meV. The propionic acids are designated A and D as found in the PDB structure file. The IUPAC nomenclature calls them respectively propionate D and C.

<sup>†</sup> This work is supported by NIH Grant RO1-GM64540.

\* To whom correspondence should be addressed. Telephone: 212-650-5557. Fax: 212-650-6940. E-mail: gunner@sci.cuny.cuny.edu.

$E_m$ s of aquo-heme  $a_3$  and  $Cu_B$  in cytochrome  $c$  oxidase have been analyzed by CE (41–43) and density functional theory (DFT) (44). DFT and QM/MM calculations have been used to explain the unusual low-spin state of ferric aquo-heme (45–47) and to study the hydroxylation mechanism (48–51) of cytochrome P450.

In the work presented here,  $pK_a$ s and  $E_m$ s of aquo-heme in myoglobins from sperm whale and *Aplysia*, hemoglobin I, heme oxygenase 1, and horseradish peroxidase are calculated with Multi-Conformation Continuum Electrostatics (MCCE) (20, 38). The calculated  $pK_a$  is compared with the pH of the acid–alkaline transition, which is attributed to the deprotonation of a water molecule as the sixth heme ligand (52). Calculations are also carried out on cytochrome  $c$  oxidase. Here the  $pK_a$  is compared with the pH dependence of the proton release on oxidation of heme  $a_3$  (53). Several of these proteins have positively charged groups in the active site. The interaction of the heme with these charges is compared in CE and DFT methods, showing that CE overestimates the interaction. With the appropriate corrections, MCCE calculations reproduce the experimental  $pK_a$ s and  $E_m$ s, showing how the protein structures yield the observed in situ reaction energetics. The differences in the shifts of aquo-heme  $pK_a$ s and  $E_m$ s in different binding sites show that electron and proton transfers can be coupled to different active site conformational changes. The aquo-heme  $E_m$  is not a factor in the function of myoglobin or hemoglobin, nor are the  $pK_a$ s important for the reaction mechanism of most of the proteins studied here. However, the aquo-heme  $pK_a$  in cytochrome  $c$  oxidase appears to determine whether heme  $a_3$  binds a proton during the reduction of the binuclear center (43). Thus, this  $pK_a$  helps to control the electroneutrality of the oxidase reduction. The comparison of calculated and measured  $pK_a$ s and  $E_m$ s in the smaller and simpler proteins provides a benchmark for the analysis of the more puzzling oxidase system.

## METHODS

Structures of sperm whale myoglobin (1A6G, 1A6K, 1A6M, 1A6N, 1HJT, 1JP6, and 1JP9), *Aplysia* myoglobin (1MBA and 5MBA), monomeric clam hemoglobin I (1B0B, 1EBT, 1FLP, and 1MOH), rat heme oxygenase 1 (1DVE, 1IVE, 1IX4, 1ULX, and 1VGI), horseradish peroxidase (1ATJ, 1H55, 1H57, 1H58, 1H5A, 1H5C, 1H5D, 1H5E, 6ATJ, and 7ATJ), and *Rhodobacter sphaeroides* cytochrome  $c$  oxidase (1M56) were obtained from the Protein Data Bank (54). All crystal waters are deleted and protein cavities filled with continuum water. Multi-Conformation Continuum Electrostatics (MCCE) samples both residue ionization state and rotamer position as a function of pH and  $E_h$  (55–57). The cytochrome  $c$  oxidase calculations use the model generated for analysis of proton uptake coupled to anaerobic reduction in MCCE2.0 (43). In this larger protein a rotation angle of  $120^\circ$  is used to make side chain rotamers, reducing the number of conformers. All other calculations use MCCE 2.2, which adds local optimization of side chain positions, pruning to delete energetically indistinguishable conformers and corrections of the CE energy terms for the errors in the dielectric boundary due to extra surface conformations (see [www.sci.ccnycunyu.edu/~mcce](http://www.sci.ccnycunyu.edu/~mcce)). Preselected side chain rotamers are generated in  $60^\circ$  increments around each rotatable bond for all amino acids. In each protein, a water or hydroxyl

is added to the open heme coordinate position. The aquo-oxygen is placed on the heme iron with square bipyramidal geometry and a 1.95 Å Fe–O bond length. Hydrogens are added in a tetrahedral geometry with a 0.96 Å H–O bond length. Then additional hydroxyl and water conformations are generated in  $30^\circ$  increments around the Fe–O bond, creating 12 conformers for both water and hydroxyl.

Look-up tables are calculated for electrostatic and non-electrostatic conformer self and conformer–conformer pairwise interactions. The electrostatic pairwise interactions and reaction field energies are determined with a finite-difference technique to solve the Poisson–Boltzmann equation using the program DelPhi (58–60). Focusing (61) is used to ensure a final grid spacing of  $>2$  grids/Å. The protein residues are given PARSE charges and radii (62). The protein has a dielectric constant,  $\epsilon$ , of 4 while the surrounding water has an  $\epsilon$  of 80 with a salt concentration of 150 mM. Cytochrome  $c$  oxidase is surrounded by a 32 Å slab with  $\epsilon = 4$  placed with IPECE to bury the fewest ionizable residues to simulate the membrane (63). The Lennard-Jones interactions are calculated with AMBER parameters (64), rescaled by 0.25 (65). A metal-centered charge set is used for hemes with a +2 or +3 charge on the ferrous and ferric Fe and –0.5 on each N atom of the porphyrin as used previously in cytochrome benchmark calculations (20, 21). The water-heme ligand uses TIP3 charges, and the hydroxyl charge, calculated with B3LYP (66) in Gaussian98 (67), has +0.2 on H and –1.2 on O. For the  $a$ -type heme in cytochrome  $c$  oxidase, a +0.3 charge is placed on the formyl group C and –0.3 on O.

MCCE calculates the shift in  $pK_a$  or  $E_m$  when a group is moved from aqueous solution to the protein. The solution  $pK_a$  ( $pK_{a,sol}$ ) and  $E_m$  ( $E_{m,sol}$ ) are obtained from measurements in water.  $pK_{a,sol}$  for amino acids are taken from studies of peptides (68, 69). The heme propionic acids are treated as described previously with a  $pK_{a,sol}$  of 4.9 (20). The five-coordinate hemes are assumed to bind a water or hydroxide as the sixth ligand. Heme and its His and water or hydroxide ligands are treated as a complex. A  $pK_{a,sol}$  of 9.6 for the hydroxyl in the ferric (70, 71) and 10.9 in the ferrous (71) His–aquo–heme has been measured in microperoxidase 8 (MP8) which has a heme  $c$ . The water  $pK_{a,sol}$ s are assumed to be the same for hemes  $a$  and  $c$ . The  $E_{m,sol}$  for the His–water heme is –120 mV, and –200 mV (72) for the His–hydroxyl heme. The value of –120 mV is slightly higher than the measured value of –140 mV (72, 73), giving an 80 mV shift from His–hydroxyl, consistent with the 1.3  $pK_a$  shift between the  $pK_a$ s of ferric and ferrous aquo–heme (70, 71). With the same ligands, the  $E_m$  of heme  $a$  is 100 (71) to 160 (74, 75) mV more positive than that of heme  $c$ . An  $E_{m,sol}$  of –20 mV for His–water heme  $a_3$  and –100 mV for His–hydroxyl heme  $a_3$  is used here. No explicit pairwise interactions of water or hydroxide ligands with the His ligand or heme to which they are bound are considered since these interactions are included in  $E_{m,sol}$  and  $pK_{a,sol}$ . The reaction field energies in both solution and the protein were calculated for the aquo–heme complexes. A systematic shift of –0.74  $\Delta pK$  unit (–1 kcal/mol) is added to the reference reaction field energy of ferric hydroxyl–heme in the solution ( $\Delta G_{RX-N,sol}$ ) and 0.5  $\Delta pK$  unit (0.67 kcal/mol) to that of ferrous water–heme. This raises all ferric heme  $pK_a$ s by 0.74 pH unit and raises the aquo–heme  $E_m$ s by 30 mV. Systematic

shifts are also applied to the ionized form of ionizable amino acids on the basis of  $pK_a$  benchmark studies (43, 56, 65).

Possible microstates with different ligand and side chain position and protonation states are subjected to Monte Carlo sampling. A microstate is made up of one conformer for each residue, cofactor, and water. The energy of microstate  $n$  ( $\Delta G^n$ ) is the sum of the electrostatic and nonelectrostatic energies (20):

$$\Delta G^n = \sum_{i=1}^M \delta_i \{ [2.3m_i k_b T (\text{pH} - pK_{\text{sol},i}) + n_i F (E_h - E_{\text{m},\text{sol},i})] + (\Delta\Delta G_{\text{rxn},i} + \Delta G_{\text{pol},i}) \} + \sum_{i=1}^M \delta_i \sum_{j=i+1}^M \delta_j [\Delta G_{ij}] \quad (1)$$

where the summation is over the total  $M$  conformers of all residues in the protein; for each conformer  $i$ ,  $\delta_i = 1$  if it is present in the current microstate  $n$  and 0 if it is not. Each residue has one conformer with  $\delta_i = 1$  and the rest  $\delta_i = 0$ . In the double summation  $\delta_i$  and  $\delta_j$  are both 1 only when conformer  $i$  and  $j$  are from two different residues.  $k_b T$  is 0.59 kcal/mol (25.8 meV), and  $m_i$  is 1 for bases,  $-1$  for acids, and 0 for polar groups and waters.  $n_i$  is the number of electrons gained or lost compared to the ground state conformer. For example, if an oxidized conformer is defined as the ground state, it has  $n_i = 0$  and the reduced conformer has  $n_i = 1$ ;  $F$  is the Faraday constant.  $pK_{\text{sol},i}$  is the  $pK_a$  and  $E_{\text{m},\text{sol},i}$  the midpoint potential of the  $i$ th cofactor in solution.  $\Delta\Delta G_{\text{rxn},i}$  is the difference between the conformer reaction field energy in solution and in the protein (desolvation energy).  $\Delta G_{\text{pol},i}$  is the pairwise electrostatic and nonelectrostatic interaction of the conformer with the backbone and with side chains that have no conformational degrees of freedom. The torsion energy for each conformer is added to  $\Delta G_{\text{pol},i}$ .  $\Delta G_{ij}$  is the electrostatic and Lennard-Jones pairwise interaction between each pair of conformers in the microstate. The limits on the summation of the interconformer terms ensure that each interaction is counted once. Monte Carlo sampling establishes the Boltzmann distribution of the different conformers of each residue at 25 °C. Residue  $pK_a$ s and  $E_m$ s are determined from the fraction group ionization in a series of Monte Carlo simulations at different pHs or  $E_h$ s (eq 1). Multiflip (76) between closely coupled residues is implemented (63). The SOFT function is not used (56). For  $pK_a$  calculations the heme is fixed in its oxidized state, and the probability of residue protonation, including that of the aquo–heme, is determined as a function of pH (56). For  $E_m$  calculations the pH is fixed at 7 and the  $E_h$  varied. All groups are allowed to sample different protonation states throughout the heme titration.

*Analysis of the MCCE  $pK_a$ s and  $E_m$ s.* The  $E_m$  or  $pK_a$  changes on moving a group from solution to its position in the protein. Thus

$$pK_a = pK_{\text{a},\text{sol}} - m\Delta\Delta G_{\text{protein}} \quad (2)$$

where  $pK_a$  is the group  $pK_a$  in the protein,  $m$  is  $-1$  for an acid and  $+1$  for a base, and

$$E_m = E_{\text{m},\text{sol}} - \Delta\Delta G_{\text{protein}}/nF \quad (3)$$

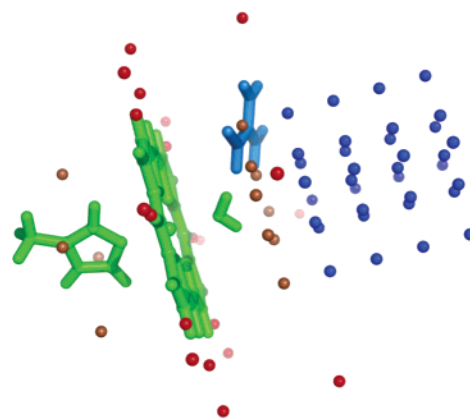


FIGURE 1: Position of external charges for comparison of CE and DFT interactions. Blue points are near the heme face; red points are in the plane of the heme and near the heme edge. Those within 4 Å of the heme plane are in brown. His–aquo–heme is in green. The position of Arg 38 in horseradish peroxidase is shown in blue.

where  $E_m$  is the heme in situ  $E_m$  and  $n$  is the number of electrons. The shift in energy of ionization ( $\Delta\Delta G_{\text{protein}}$ ) is due to different changes of the reaction reactant and product energies when the reaction is moved into the protein. This term can be broken down in MCCE into the sum:

$$\Delta\Delta G_{\text{protein}} = (\Delta\Delta G_{\text{rxn}} + \Delta G_{\text{pol}}) + \Delta G_{\text{res}} \quad (4)$$

including the change in reaction field energy from solution ( $\Delta\Delta G_{\text{rxn}}$ ), the added interaction with the rigid backbone ( $\Delta G_{\text{pol}}$ ), and the side chains in their ionization and conformational states equilibrated at the given pH and  $E_h$  ( $\Delta G_{\text{res}}$ ) (20, 43, 77).

MCCE uses continuum electrostatics to calculate the interaction between the aquo–heme and charges and dipoles in the protein. Selected interactions with the ferric heme porphyrin together with its imidazole and water or hydroxyl ligand were also calculated using Gaussian 98 (67). The heme and imidazole are taken from the crystal structure of sperm whale myoglobin (1A6K), with water or hydroxyl added in GaussView (67). Each structure is then optimized using the B3LYP method (66) with the LANL2DZ basis set (78). Hydroxyl–hemes are expected to be low spin (53, 79) while water–hemes are generally high spin (53, 80). The water–heme is given a net charge  $+1$  and spin  $5/2$ , while the hydroxyl–heme has a net charge 0 and spin  $1/2$ . The change in system energy is then calculated with an external charge of  $+1$  or  $-1$  placed next to the aquo–heme complex in positions shown in Figure 1. All atoms are fixed in the structure optimized before the charge is added.

Nine external charges are placed on a plane parallel to the porphyrin plane located 4, 6, 8, 10, or 12 Å from the heme (Figure 1). Points that overlap the water or imidazole ligand are removed. The interactions are also calculated with Coulomb's law with the metal-centered charges used in the MCCE calculations with  $\epsilon = 1$ . For the ferric hydroxyl–heme, Coulomb's law reproduces the DFT interactions with an error of  $<10\%$  and a slope of 0.94 with the exception of points within 4 Å of the heme plane (Figure 2). However, for the water–heme, the Coulomb's law interactions with the points above the heme plane are significantly larger than those obtained with DFT. In contrast, for charges on the heme

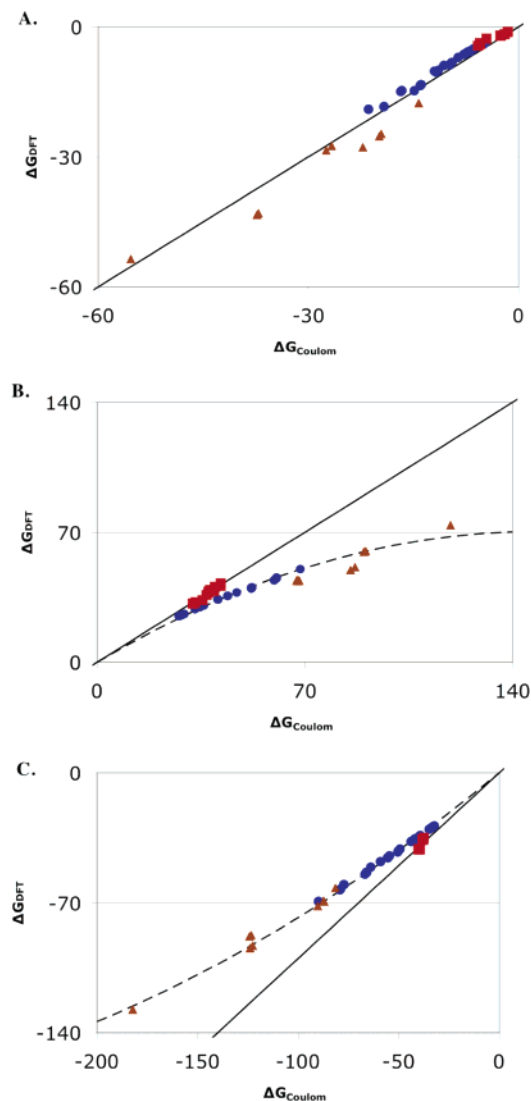


FIGURE 2: Comparison of interactions with a positive charge (blue ●) near the heme face, (red ■) in the plane of the heme and near the heme edge, and (brown ▲) within 4 Å of the heme plane as shown in Figure 1 calculated with DFT or CE Coulomb's law with  $\epsilon = 1$ . (A) Neutral, ferric (hydroxyl-heme). The ideal straight line through the origin with a slope of 1 is shown. (B) Cationic, ferric water-heme. The line through the points,  $y = 0.95x - (3.2 \times 10^{-3})x^2$ , is the best fit to a binomial function for the points near the heme face (blue). (C) (Hydroxyl-heme) - (water-heme). The line through the points is  $y = 0.89x + (1.1 \times 10^{-3})x^2$ .

edge (Figure 1) the Coulomb's law interactions reproduce the DFT interactions with <5% error and a slope of 1.0 for both water and hydroxyl ligated hemes (Figure 2). The source of the error in the CE calculation is not known. However, the large unfavorable interactions with water-heme are relaxed in the DFT calculations, while the smaller, favorable interactions with hydroxyl-heme are not. This suggests that there is significantly more polarization of the ferric water-heme by the external charge. In addition, the correction could be needed if there is significant charge at positions that are not well described by the atom-centered charges used here. Further studies are in progress to develop a water-heme charge distribution, perhaps including charges out of the heme plane, which can better reproduce the DFT interaction with Coulomb's law. Preliminary calculations show that in general there is no systematic error in the CE calculations

of the interactions of the standard amino acids with external charges.

The ferric water-heme interaction of a simple external charge at the position of Arg 38 in peroxidase or  $\text{Cu}_B$  in oxidase calculated with DFT is only 60% of that found with Coulomb's law. The interaction with a charge at the position of Arg 99 in hemoglobin I is 65% as large. The influence of the charge distribution for the external group on the correction was examined by using a PARSE Arg charge distribution, rather than a single +1 charge. The DFT interaction is now 63% of that found with Coulomb's law, very similar to that found with a unitary charge model. The influence of the charge distribution of  $\text{Cu}_B$  is more complex and cannot be described by a simple scaling factor. The details are discussed in ref 43.

Corrections are applied to interactions of the water-heme with Arg 99 in hemoglobin, Arg 38 in peroxidase, and  $\text{Cu}_B$  in oxidase. However, pairwise electrostatic interactions in MCCE are calculated with the Poisson-Boltzmann equation (PB), a CE analysis which takes into account the different dielectric constants of the protein and water (30, 81). The scaling factor derived for particular heme-residue geometry from the comparison of Coulomb's law and DFT interactions in a vacuum (Figure 2) is used to scale the individual PB interactions in MCCE. Corrections used for  $\text{Cu}_B$  can be found in ref 43.

Interactions with residues that are on the heme plane or far away from the heme are shown to need no correction. Residues that have significant interactions with the aquo-heme which are not corrected because of their position include the following: all of the heme propionates; Arg 45 which is hydrogen bonded to a propionic acid in myoglobin; Lys 179 which is hydrogen bonded to a propionate in hemoglobin I; Arg 136 and Asp 140 which form an ion pair on the porphyrin edge furthest from the propionates in hemoglobin I (Figure 4).

## RESULTS AND DISCUSSION

The ferric aquo-heme  $\text{pK}_a$ s were calculated with MCCE in myoglobins from sperm whale and *Aplysia*, hemoglobin I, heme oxygenase 1, horseradish peroxidase, and cytochrome *c* oxidase and compared to measured values. These  $\text{pK}_a$ s span 3.3 pH units from 7.6 in heme oxygenase 1 to 10.9 in the peroxidase. Two sets of calculations are presented. In the first set, standard Poisson-Boltzmann continuum electrostatics (CE) calculations are used for all pairwise interactions between the aquo-heme and the surrounding protein residues. In the second, an additional correction derived from DFT calculations is applied. Calculated  $\text{pK}_a$ s are compared to the experimental values. Calculations of the heme  $E_m$ s are discussed below.

The  $\text{pK}_a$ s calculated using the standard CE-based pairwise interactions in MCCE (20) do not provide consistent agreement with the experimental data (Figure 3). Calculated  $\text{pK}_a$ s for the myoglobins and heme oxygenase are within 1 pH unit of the measured values. However, errors as large as 6 pH units are found in horseradish peroxidase and cytochrome *c* oxidase. In these proteins a nearby positive charge in the heme distal pocket lowers the calculated  $\text{pK}_a$ , while the myoglobins have no charges in similar positions. As described in the Methods section CE and DFT calculations

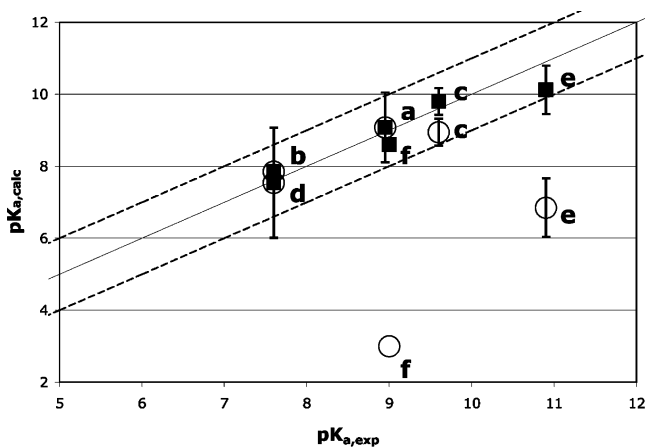


FIGURE 3: Comparison of calculated and experimental  $pK_a$ s (■) with and (○) without the DFT correction for (a) sperm whale myoglobin, (b) *Aplysia* myoglobin, (c) hemoglobin I, (d) heme oxygenase, (e) horseradish peroxidase, and (f) cytochrome *c* oxidase. The ideal line of slope 1 passing through the origin and lines with differences between experimental and calculated of  $\pm 1$  pH unit (dashed lines) are shown. References for experimental values are in Table 1.

provide very similar values for pairwise interactions between a charge and a neutral hydroxyl–heme, probably because the electronic polarization does not contribute much to this smaller, favorable interaction. For the cationic water–heme, both methods also yield similar results when the charge is on the heme edge. However, when the charge is above the heme plane near the iron, the interactions derived with a CE analysis are significantly larger than those obtained with DFT calculations. The closer the charge is to the heme plane, the larger the discrepancy (Figure 2). The large unfavorable interactions are relaxed when electronic polarization is considered in the DFT calculations. The DFT corrections are applied to the pairwise electrostatic interaction of the water–heme with Arg 99 in hemoglobin I, Arg 38 in horseradish peroxidase, and  $Cu_B$  in cytochrome *c* oxidase to recalculate the  $pK_a$ s. Now calculated  $pK_a$ s in the six proteins agree with the measured values within 1 pH unit. Analysis of the MCCE calculations can then show how interactions and conformational changes shift the  $pK_{a,sol}$  of 9.6 to different in situ values in these proteins.

**Sperm Whale Myoglobin.** Sperm whale myoglobin has a folded six-helix core (Figure 4). The  $pK_a$  of the ferric aquo–heme is 8.95 (52), little different from the  $pK_{a,sol}$  of 9.6. MCCE calculations with seven different crystal structures give an average aquo–heme  $pK_a$  of  $9.1 \pm 1.0$ , in good agreement with experiment. This heme is close to the protein surface. However,  $pK_a \approx pK_{a,sol}$  not because the heme does not interact with the protein but rather because a number of effects cancel (Table 1). The water–heme, with a net +1 charge, has 7  $\Delta pK$  units (9.52 kcal/mol) less solvation energy in the protein than it does in water, but the hydroxyl–heme, which has a large dipole moment, has a 5  $\Delta pK$  unit desolvation energy. Thus, the resultant desolvation penalty ( $\Delta\Delta G_{rxn}$ ) favors the water–heme complex raising the  $pK_a$  by about 2 pH units. The backbone amide dipoles tend to raise the electrostatic potential within all proteins, shifting residue  $pK_a$ s (25, 82) and cytochrome *E<sub>m</sub>S* (20). Here they favor the hydroxyl–heme, lowering the  $pK_a$  by 1 pH unit. The E helix, which contains His 64 in the distal pocket, is the largest contributor.

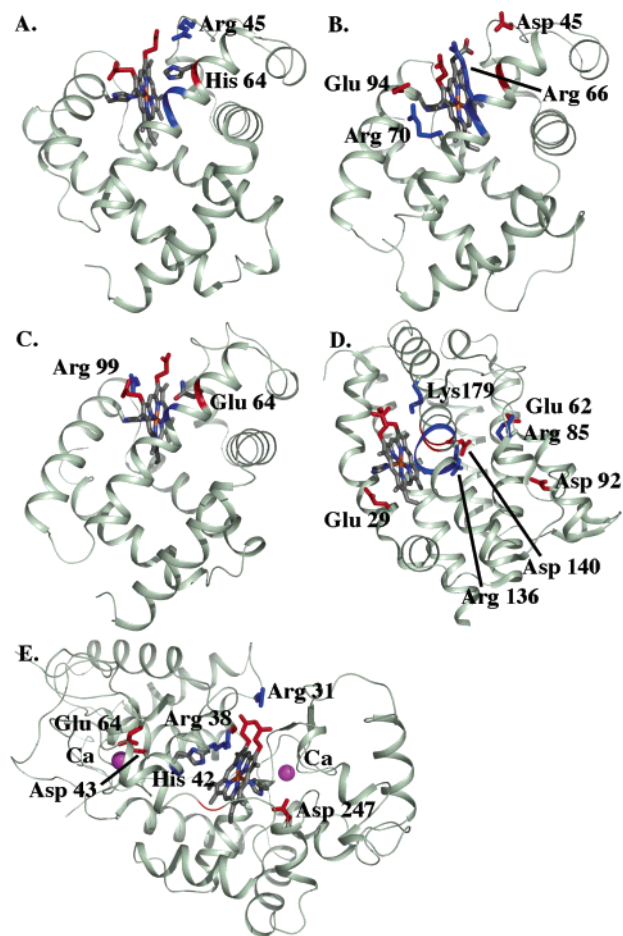


FIGURE 4: Structures of (A) sperm whale myoglobin, (B) *Aplysia* myoglobin, (C) hemoglobin I, (D) heme oxygenase, and (E) horseradish peroxidase. Residues and backbone segments that interact with the cationic ferric aquo–heme by more than 0.5  $\Delta pK$  unit (0.68 kcal/mol) are shown.

There are 4 Arg, 14 Glu, 7 Asp, and 19 Lys in the protein and all of them are >95% ionized between pH 7 and pH 9. However, most of these charges have little effect on the aquo–heme  $pK_a$  because they are solvent exposed. Arg 45, which is hydrogen-bonded to the D-ring propionic acid, does shift the  $pK_a$  down by 0.6  $pK$  unit (propionate A and D designated as assigned in the PDB structure files). The two heme propionic acids are both fully ionized and together shift the  $pK_a$  up by 2.3 units. As these are all near the heme edge, the CE interaction agrees with the DFT values (Figure 2). His 64 in the distal heme pocket near the aquo–ligand undergoes a conformational change with the change in the aquo–heme protonation state (Figure 4). The His is always neutral, but the  $\delta$  proton tautomer stabilizes the positive water–heme by 3–4  $\Delta pK$  units, while the protonated  $\epsilon$  tautomer stabilizes the hydroxyl–heme by 1.6–2.5  $\Delta pK$  units. In different PDB structures the His tautomer is restricted by the rigid backbone to different extents, yielding the dependence of the calculated  $pK_a$  on the starting structure. Arg 45 not only lowers the aquo–heme  $pK_a$  by direct electrostatic interaction but it also lowers the  $pK_a$  indirectly by favoring the  $\epsilon$  His 64 conformer.

***Aplysia* Myoglobin.** Myoglobin from the sea hare *Aplysia limacina* has a folded six-helix structure (Figure 4). It is calculated to have a ferric aquo–heme  $pK_a$  of 7.7, 2  $pK$  units lower than that of sperm whale myoglobin, in agreement

Table 1: Experimental and Calculated  $pK_a$ s and  $E_m$ s and Energy Terms Contributing to  $pK_a$  and  $E_m$  Shifts in the Protein

(a) $pK_a$ of Ferric Aquo-heme					
	exp $pK_a$	MCCE $pK_a$	$\Delta\Delta G_{rxn}$ ( $\Delta pK$ unit)	$\Delta G_{pol}$ ( $\Delta pK$ unit)	$\Delta G_{res}$ ( $\Delta pK$ unit)
sperm whale myoglobin (7) <sup>a</sup>	8.95 (52)	9.1 $\pm$ 1.0	2.07 $\pm$ 0.29	0.91 $\pm$ 0.14	-2.45 $\pm$ 0.83
<i>Aplysia</i> myoglobin (2)	7.6 (52)	7.7 $\pm$ 1.0	1.70 $\pm$ 0.34	0.88 $\pm$ 0.23	-0.75 $\pm$ 0.49
hemoglobin I (4)	9.6 (83)	9.8 $\pm$ 0.3	1.30 $\pm$ 0.18	1.02 $\pm$ 0.09	-2.57 $\pm$ 0.24
heme oxygenase 1 (5)	7.6 (84, 85)	7.5 $\pm$ 1.5	0.16 $\pm$ 0.37	3.34 $\pm$ 0.69	-1.44 $\pm$ 1.10
horseradish peroxidase (10)	10.9 (52)	10.1 $\pm$ 0.7	1.58 $\pm$ 0.39	-0.61 $\pm$ 0.07	-1.49 $\pm$ 0.66
cyt <i>c</i> oxidase (1)	9.0 (53)	8.6	3.9	0.4	-3.3
(b) $E_m$ of Aquo-heme at pH 7					
	exp $E_m$ (mV)	MCCE $E_m$ (mV)	$\Delta\Delta G_{rxn}$ ( $\Delta pK$ unit)	$\Delta G_{pol}$ ( $\Delta pK$ unit)	$\Delta G_{res}$ ( $\Delta pK$ unit)
sperm whale myoglobin (7)	50 (86)	25 $\pm$ 33	4.50 $\pm$ 0.56	0.98 $\pm$ 0.15	-2.97 $\pm$ 0.66
<i>Aplysia</i> myoglobin (2)	125 (86)	126 $\pm$ 64	4.25 $\pm$ 1.24	0.89 $\pm$ 0.11	-0.89 $\pm$ 0.24
hemoglobin I (4)	103 (87)	83 $\pm$ 15	4.33 $\pm$ 0.17	0.85 $\pm$ 0.12	-1.68 $\pm$ 0.09
heme oxygenase 1 (5)	NA	37 $\pm$ 13	2.47 $\pm$ 0.36	1.84 $\pm$ 0.44	-1.61 $\pm$ 0.30
horseradish peroxidase (10)	-250 (88, 89)	-215 $\pm$ 27	3.80 $\pm$ 0.51	-0.62 $\pm$ 0.06	-4.79 $\pm$ 0.49
cyt <i>c</i> oxidase <sup>b</sup> (1)	NA	9	5.77	0.77	-5.70

<sup>a</sup> The value in parentheses is the number of PDB files analyzed. NA, not available. Negative free energy terms favor the cationic ferric water-heme raising the aquo-heme  $pK_a$  and favor the oxidized heme lowering the  $E_m$ . The ferric aquo-heme  $pK_{a,sol}$  is 9.6 (70, 71). The *b*-type water-hemes have an  $E_{m,sol}$  of -120 mV, while the *a*-type heme in cytochrome *c* oxidase has an  $E_{m,sol}$  of -20 mV. Hydroxyl-hemes have  $E_{m,sols}$  80 mV lower than the water-hemes (72, 73), consistent with the 1.3  $pK_a$  unit shift between the  $pK_a$ s of ferric and ferrous aquo-heme (70, 71). <sup>b</sup> The  $pK_a$  and  $E_m$  of the aquo-heme  $a_3$  is calculated with  $Cu_A$  oxidized and heme *a* and  $Cu_B$  reduced to mimic the experimental  $pK_a$  measurements in the CO photolyzed mixed-valence complex (53). 1  $\Delta pK$  unit = 58 meV = 1.36 kcal/mol. A systematic shift of -0.74  $\Delta pK$  unit (-1 kcal/mol) is added to the reference reaction field energy ( $\Delta\Delta G_{RXN,sol}$ ) of ferric hydroxyl-heme and 0.5  $\Delta pK$  unit (0.67 kcal/mol) to ferrous water-heme in deriving the in situ  $E_m$ s and  $pK_a$ s using eqs 2-4.

with the experimental value of 7.6 (52). The *Aplysia* and sperm whale proteins have the same protein folds and are 27% identical. The analogue of myoglobin His 64 is Val 64 in the *Aplysia* distal pocket, providing a bigger cavity, so the heme is slightly better solvated, shifting the  $pK_a$  up. However, the biggest difference between the two proteins is in  $\Delta G_{res}$ . The loss of His 64 and protonation of the ring D propionic acid lowers the aquo-heme  $pK_a$ . The propionate  $pK_a$  is raised to 8.6 by the nearby Asp 45, while in myoglobin Arg 45 lowers the propionate  $pK_a$  to 4.6.

**Hemoglobin I.** Monomeric clam hemoglobin I also has a folded six-helix structure (Figure 4). The aquo-heme  $pK_a$  is calculated to be 9.8 and measured to be 9.6 (83), close to that of sperm whale myoglobin. The hemoglobin I and myoglobin have similar structures with 23% identity. A larger cavity in the heme distal pocket leads to a smaller desolvation energy. As His 64 does in myoglobin, Gln 64 changes conformation, keeping its oxygen pointing toward the water-heme and nitrogen pointing toward the hydroxyl-heme. Arg 99, on the proximal side of the heme, shifts the  $pK_a$  down by 1.5 pH units, while the two propionic acids, both of which are ionized, shift the  $pK_a$  up by 2.2 pH units.

**Heme Oxygenase 1.** Rat heme oxygenase 1 is a multi-helical bundle with two three-helix motifs (Figure 4). The aquo-heme  $pK_a$  is calculated to be 7.5, in agreement with the experimental value of 7.6 (84, 85). In this protein heme is an exchangeable substrate and is significantly more exposed than in the other proteins considered here and so has a very small  $\Delta\Delta G_{rxn}$ . The large positive potential from the backbone lowers the  $pK_a$  by 3.3 pH units. The distal pocket helix is kinked at Gly 143 and Gly 144 so the backbone amides of Ser 142, Gly 143, and Gly 144 all point toward the heme iron, stabilizing the hydroxyl-heme. Arg 136 and Asp 140 are in a salt bridge near the porphyrin edge. While each interacts with the aquo-heme by over 3  $\Delta pK$  units, their combined impact is small.

**Horseradish Peroxidase.** The multi-helical peroxidase uses heme to reduce hydrogen peroxide to water. The aquo-heme  $pK_a$  is calculated to be 10.1, in reasonable agreement with the measured 10.9 (52). The aquo-heme has a similar reaction field energy loss as the globins. Unlike the globins, interactions with the backbone amides near the metal center are small and somewhat negative, raising the  $pK_a$  by 0.6 pH unit. Interactions with other residues raise the  $pK_a$  by 1.5  $\Delta pK$  units. His 42 and Asp 43 raise the  $pK_a$  by 6 pH units while Arg 38 shifts the  $pK_a$  down by 4.5 pH units (assuming a 60% DFT correction). His 42 sits in the distal pocket in a position similar to His 42 in myoglobin. However, this His is fixed in the  $\delta$  tautomer by Arg 38, Glu 64, and Asn 70, stabilizing the protonated water-heme.

**Cytochrome *c* Oxidase.** Heme  $a_3$  in cytochrome *c* oxidase is deeply buried in the transmembrane 12-helix subunit I of the protein. In the mixed-valence state, with heme *a* and  $Cu_B$  reduced, the ferric aquo-heme  $pK_a$  has been measured to be 9 (53). Using the full CE interaction between  $Cu_B$  and the aquo-heme, the calculated  $pK_a$  is 3. The DFT correction reduces the interaction from 6.4 to 3.2  $\Delta pK$  units. Since the aquo-heme titration now occurs at higher pH, the protein net charge is more negative than when the titration is at pH 3. This raises the  $pK_a$  further to 8.6, in good agreement with experiment (43). The cytochrome *c* oxidase heme is more deeply buried than in the other proteins, losing more reaction field energy, which shifts the  $pK_a$  down. Within the membrane-embedded protein, pairwise electrostatic interactions with other residues are quite long range. However, the net interaction of the fully ionized propionic acids and the rest of the protein shifts the  $pK_a$  up by only 2 pH units.

**$E_m$  Calculations.** The aquo-heme  $E_m$ s were calculated in each protein at pH 7.  $E_m$ s previously measured in four of the proteins range from -250 mV in peroxidase to 125 mV in *Aplysia* myoglobin (86) (Table 1b). MCCE calculations agree with the experimental values with errors of  $\leq 35$  mV.

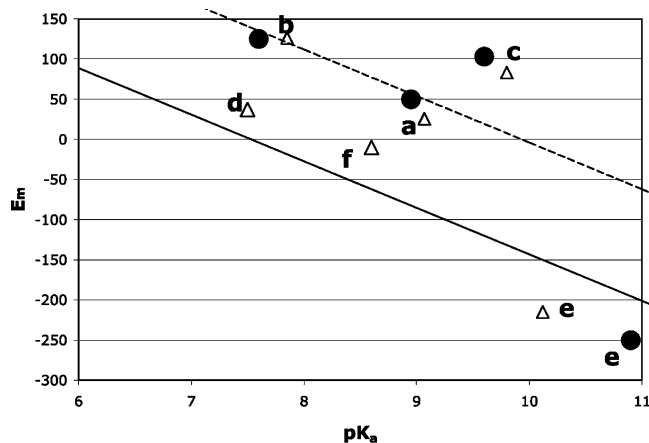


FIGURE 5:  $E_m$  versus  $pK_a$  at pH 7 for (a) sperm whale myoglobin, (b) *Aplysia* myoglobin, (c) hemoglobin I, (d) heme oxygenase, (e) horseradish peroxidase, and (f) cytochrome *c* oxidase. (Δ) Calculated and (●) available experimental values. The solid line has the same  $\Delta\Delta G_{\text{protein}}$  for the in situ  $E_m$  and  $pK_a$  (eqs 2 and 3). The dashed line of  $\Delta\Delta G_{\text{protein}}$  is 2.4  $\Delta pK$  units larger for  $E_m$  than  $pK_a$ ; 2.4  $\Delta pK$  units is the average difference in the  $\Delta\Delta G_{\text{rxn}}$  for the two types of reactions (Table 1).

MCCE allows protonation of the aquo–heme to be coupled to heme reduction (20). The relevant  $E_{m,\text{sol}}$  for water–heme of  $-120$  mV (72, 73) and for hydroxyl–heme of  $-200$  mV (72) is included in the microstate energy (eq 1) so the pH dependence of the  $E_m$  is properly treated in the redox titration. This degree of freedom could be important for *Aplysia* myoglobin and heme oxygenase, which have  $pK_a$ s near 7. However, since their ferric  $pK_a$ s are above 7 and ferrous  $pK_a$ s are higher, the aquo–heme ligand remains predominately water at pH 7.

Electrostatic interactions that favor the ferric heme with its net charge of +1 over the neutral ferrous heme shift the  $E_m$  down. The same electrostatic interactions favor the cationic ferric water–heme over the neutral hydroxyl–heme, raising the  $pK_a$ . While a higher  $pK_a$  is correlated with a lower  $E_m$ , the connection is by no means exact (Figure 5). In most proteins, the  $\Delta\Delta G_{\text{protein}}$  for the redox reaction is larger than for the protonation reaction so the  $E_m$  is shifted from  $E_{m,\text{sol}}$  by more than the  $pK_a$  is shifted from  $pK_{a,\text{sol}}$  (Figure 5, eqs 2 and 3). One difference is the desolvation energy is on average  $2.4 \pm 0.3$   $\Delta pK$  units larger for the redox reaction than for the protonation reaction (Table 1). Because of its significant dipole the solvated neutral ferric hydroxyl–heme has a solvation energy that is not much smaller than the positively charged ferric water–heme. Thus, both reactant and product of the protonation reaction have similar  $\Delta\Delta G_{\text{rxn}}$ . With the exception of cytochrome *c* oxidase, the desolvation penalty, which always favors the neutral species, shifts the  $pK_a$  down by at most 2 pH units. In contrast, when compared to the neutral, ferrous water–heme, the cationic, ferric water–heme has much larger interactions with water. The impact of the desolvation energy on the redox reaction when the heme is buried in the protein is thus much larger.

Hemoglobin I has a  $pK_a$  which is only 0.2 pH unit higher than the  $pK_{a,\text{sol}}$ , while the  $E_m$  is 223 mV more positive than  $E_{m,\text{sol}}$  ( $\Delta\Delta G_{\text{protein}} = 3.8$   $\Delta pK$  units). The difference in desolvation energy for the two reactions contributes 3  $\Delta pK$  units. In addition, Gln 64 in the distal pocket changes conformation in the aquo–heme  $pK_a$  titration but does not in the  $E_m$  titration. The rigid Gln 64 raises the water–heme

$E_m$  by 1  $\Delta pK$  unit (58 meV) more than it shifts the ferric aquo–heme  $pK_a$  down. The reorientation of the Gln is part of the protein dielectric response that is captured by the explicit motions available in MCCE (30, 55). The Gln motion coupled to aquo–heme protonation thus diminishes the effective pairwise interaction.

In horseradish peroxidase,  $\Delta\Delta G_{\text{protein}}$  shifts the  $E_m$  down more than it shifts the  $pK_a$  up. Besides the 2.2  $\Delta pK$  unit difference in the desolvation energy,  $\Delta G_{\text{res}}$  favors heme reduction 3.3  $\Delta pK$  units more than water deprotonation. Although both ferrous water–heme and ferric hydroxyl–heme have a net charge of 0, they interact differently with nearby residues. The hydroxyl–heme has a large dipole with its negatively charged hydroxide pointing toward the distal pocket. Arg 38 in the distal pocket and Asp 247 on the opposite side form a dipole stabilizing the hydroxyl–heme. The difference in interactions with hydroxyl–heme and water–heme is relatively small, leading to a small  $\Delta G_{\text{res}}$ , contributing to the  $pK_a$  shift. On the other hand, the neutral ferrous water–heme is not stabilized by the electrostatic dipole generated by these two amino acids while interactions of the ferric water–heme with nearby negative charges shift the  $E_m$  down.

As in horseradish peroxidase, the favorable interaction of  $\text{Cu}_B$  with the hydroxyl–heme in cytochrome *c* oxidase makes the contribution of  $\Delta G_{\text{res}}$  to the in situ  $pK_a$  smaller than found for in situ  $E_m$ . Assuming the  $E_{m,\text{sol}}$  of heme a is 100 (1) to 160 (74, 75) mV more positive than that of heme c, the  $E_m$  of heme a<sub>3</sub> is predicted to be 9 to 69 mV in cytochrome *c* oxidase when  $\text{Cu}_A$  is oxidized and heme A and  $\text{Cu}_B$  are reduced.

There are no experimental data available for the  $E_m$  in heme oxygenase 1. These calculations predict an  $E_m$  of 40 mV. A run of four backbone dipoles lowers the  $pK_a$  more than the  $E_m$ . All of the other proteins studied here have similar values of  $\Delta G_{\text{pol}}$  for the redox and protonation reactions.

## CONCLUSIONS

The  $pK_a$ s of ferric aquo–heme at pH 7 in sperm whale myoglobin, *Aplysia* myoglobin, hemoglobin I, heme oxygenase 1, horseradish peroxidase, and cytochrome *c* oxidase were calculated with MCCE. The calculations reveal a breakdown in the classic continuum electrostatic analysis of pairwise interactions. Large errors in calculated  $pK_a$ s were found in horseradish peroxidase and cytochrome *c* oxidase. DFT calculations suggest that CE calculations overestimate pairwise interactions between ferric water–heme and a positive charge above the heme plane. This could be due to significant out-of-plane charge density, which would be ignored in the atom-centered charges used in the CE analysis. Alternatively, these external charges could polarize ferric hydroxyl–heme significantly more than the amount accounted for by the  $\epsilon = 4$  used in the MCCE calculation. Using a correction that brings the DFT and CE interactions into agreement, the calculated  $pK_a$ s in six proteins are within 1 pH unit of the experimental values. The calculated  $E_m$ s using the correction derived from DFT calculations are within 35 mV of the experimental values.

Proteins with higher ferric aquo–heme  $pK_a$ s have lower  $E_m$ s since both arise from the protein stabilizing a positively

charged heme. However, the proteins shift the free energy of the redox reaction ( $\Delta\Delta G_{\text{protein}}$ ) by an amount that would shift a  $pK_a$  by  $>6$  pH units (375 mV), while the  $pK_a$ s span only 3.3 pH units (eqs 2 and 3). The difference in  $\Delta\Delta G_{\text{protein}}$  shows that there is a larger effective dielectric response for the protonation than the redox reactions. In sperm whale myoglobin and hemoglobin I protonation is coupled to conformational changes while the redox reaction is not. These conformational changes allow a residue in the distal pocket to stabilize both protonation states, reducing the energy difference between them. In contrast, when the group is rigid as it is for the redox reaction, the pairwise interactions are larger, shifting the  $E_m$  more. This difference in flexibility for the two reaction types found in MCCE is supported by the good match between calculation and experiment for both  $pK_a$ s and  $E_m$ s.

## ACKNOWLEDGMENT

We gratefully acknowledge helpful discussions with Ronald Koder.

## SUPPORTING INFORMATION AVAILABLE

Interactions between heme  $a_3$  and  $\text{Cu}_B$  in different aquo protonation and cofactor redox states calculated in a vacuum by Coulomb's law and by DFT using Gaussian 98 and in cytochrome  $c$  oxidase embedded in a low dielectric slab surrounded by water using DelPhi. This material is available free of charge via the Internet at <http://pubs.acs.org>.

## REFERENCES

- Reedy, C. J., and Gibney, B. R. (2004) Heme protein assemblies, *Chem. Rev.* 104, 617–649.
- Antonin, E., and Brunori, M. (1971) *Hemoglobin and Myoglobin in their Reactions with Ligands*, North-Holland, Amsterdam.
- Tenhunen, R., Marver, H. S., and Schmid, R. (1969) Microsomal heme oxygenase. Characterization of the enzyme, *J. Biol. Chem.* 244, 6388–6394.
- Welinder, K. G. (1992) Superfamily of plant, fungal and bacterial peroxidases, *Curr. Opin. Struct. Biol.* 2, 338–393.
- Smith, A. T., and Veitch, N. C. (1998) Substrate binding and catalysis in heme peroxidases, *Curr. Opin. Chem. Biol.* 2, 269–278.
- Brzezinski, P. (2004) Redox-driven membrane-bound proton pumps, *Trends Biochem. Sci.* 29, 380–387.
- Gennis, R. B. (2003) Some recent contributions of FTIR difference spectroscopy to the study of cytochrome oxidase, *FEBS Lett.* 555, 2–7.
- Ferguson-Miller, S., and Babcock, G. T. (1996) Heme/copper terminal oxidases, *Chem. Rev.* 96, 2889–2907.
- Wikstrom, M. (2004) Cytochrome  $c$  oxidase: 25 years of the elusive proton pump, *Biochim. Biophys. Acta* 1655, 241–247.
- Montfort, W. R., Weichsel, A., and Andersen, J. F. (2000) Nitrophorins and related antihemostatic lipocalins from *Rhodnius prolixus* and other blood-sucking arthropods, *Biochim. Biophys. Acta* 1482, 110–118.
- Privalle, C. T., Crivello, J. F., and Jefcoate, C. R. (1983) Regulation of intramitochondrial cholesterol transfer to side-chain cleavage cytochrome P-450 in rat adrenal gland, *Proc. Natl. Acad. Sci. U.S.A.* 80, 702–706.
- Pikuleva, I., and Waterman, M. (1999) Cytochromes P450 in synthesis of steroid hormones, bile acids, vitamin D3 and cholesterol, *Mol. Aspects Med.* 20, 33–42, 43–37.
- Rodgers, K. R. (1999) Heme-based sensors in biological systems, *Curr. Opin. Chem. Biol.* 3, 158–167.
- Chan, M. K. (2001) Recent advances in heme-protein sensors, *Curr. Opin. Struct. Biol.* 5, 216–222.
- Churg, A. K., and Warshel, A. (1986) Control of the redox potential of cytochrome  $c$  and microscopic dielectric effects in proteins, *Biochemistry* 25, 1675–1681.
- Poulos, T. L. (1988) Heme enzyme crystal structure, *Heme Proteins: Struct., Funct., Genet.* 7, 2–36.
- Rietjens, I. (1996) The role of the axial ligand in heme-based catalysis, *J. Biol. Inorg. Chem.* 1, 355.
- Martin, A. C. R., Orengo, C. A., Hutchinson, E. G., Jones, S., Karmirantzou, M., Laskowski, R. A., Mitchell, J. B. O., Taroni, C., and Thornton, J. M. (1998) Protein folds and function, *Structure* 6, 875–884.
- Stellwagen, E. (1978) Haem exposure as the determinate of oxidation–reduction potential of haem proteins, *Nature* 275, 73–74.
- Mao, J., Hauser, K., and Gunner, M. R. (2003) How cytochromes with different folds control heme redox potentials, *Biochemistry* 42, 9829–9840.
- Gunner, M. R., and Honig, B. (1991) Electrostatic control of midpoint potentials in the cytochrome subunit of the *Rhodospseudomonas viridis* reaction center, *Proc. Natl. Acad. Sci. U.S.A.* 88, 9151–9155.
- Voigt, P., and Knapp, E. W. (2003) Tuning heme redox potentials in the cytochrome  $c$  subunit of photosynthetic reaction centers, *J. Biol. Chem.* 278, 51993–52001.
- Kassner, R. J. (1973) A theoretical model for the effects of local nonpolar heme environments on the redox potentials in cytochromes, *J. Am. Chem. Soc.* 95, 7959–7975.
- Kassner, R. J. (1972) Effects of nonpolar environments on the redox potentials of heme complexes, *Proc. Natl. Acad. Sci. U.S.A.* 69, 2263–2267.
- Kim, J., Mao, J., and Gunner, M. R. (2005) Are acidic and basic groups in buried proteins predicted to be ionized?, *J. Mol. Biol.* 348, 1283–1298.
- Muegge, I., Qi, P. X., Wand, A. J. W., Chu, Z. T., and Warshel, A. (1997) The reorganization energy of cytochrome  $c$  revisited, *J. Phys. Chem.* 101, 825–836.
- Churg, A. K., Weiss, R. M., Warshel, A., and Takano, T. (1983) On the action of cytochrome  $c$ : correlating geometry changes upon oxidation with activation energies of electron transfer, *J. Phys. Chem.* 87, 1683–1694.
- Cutler, R. L., Davies, A. M., Creighton, S., Warshel, A., Moore, G. R., Smith, M., and Mauk, A. G. (1989) Role of arginine-38 in regulation of the cytochrome  $c$  oxidation–reduction equilibrium, *Biochemistry* 28, 3188–3197.
- Warwicker, J., and Watson, H. C. (1982) Calculation of the electric potential in the active site cleft due to a  $\alpha$ -helix dipoles, *J. Mol. Biol.* 157, 671–679.
- Gunner, M. R., and Alexov, E. (2000) A pragmatic approach to structure based calculation of coupled proton and electron transfer in proteins, *Biochim. Biophys. Acta* 1458, 63–87.
- Zhou, H. X. (1997) Control of reduction potential by protein matrix: lesson from a spherical protein model, *J. Biol. Inorg. Chem.* 2, 109–113.
- Warshel, A., Papazyan, A., and Muegge, I. (1997) Microscopic and semimacroscopic redox calculations: what can and can not be learned from continuum models, *J. Biol. Inorg. Chem.* 2, 143–152.
- Baptista, A. M., Martel, P. J., and Peterson, S. B. (1997) Simulation of protein conformational freedom as a function of pH: constant-pH molecular dynamics using implicit titration, *Proteins: Struct., Funct., Genet.* 27, 523–544.
- Soares, C. M., Martel, P. J., Mendes, J., and Carrondo, M. A. (1998) Molecular dynamics simulation of cytochrome  $c_3$ : studying the reduction processes using free energy calculations, *Biophys. J.* 74, 1708–1721.
- Baptista, A., Martel, P. J., and Soares, C. M. (1999) Simulation of electron–proton coupling with a Monte Carlo method: application to cytochrome  $c_3$  using continuum electrostatics, *Biophys. J.* 76, 2978–2998.
- Martel, P. J., Soares, C. M., Baptista, A. M., Fuxreiter, M., Naray-Szabo, G., Louro, R. O., and Carrondo, M. A. (1999) Comparative redox and  $pK_a$  calculations on cytochrome  $c_3$  from several *Desulfovibrio* species using continuum electrostatic methods, *J. Biol. Inorg. Chem.* 4, 73–86.
- Zaric, S. D., Popovic, D. M., and Knapp, E. W. (2001) Factors determining the orientation of axially coordinated imidazoles in heme proteins, *Biochemistry* 40, 7914–7928.
- Haas, A. H., and Lancaster, C. R. (2004) Calculated coupling of transmembrane electron and proton transfer in dihemic quinol: fumarate reductase, *Biophys. J.* 87, 4298–4315.
- Rogers, N. K., Moore, G. R., and Sternberg, M. J. E. (1985) Electrostatic interactions in globular proteins: Calculation of the



- pH dependence of the redox potential of cytochrome *c*<sub>551</sub>, *J. Mol. Biol.* **182**, 613–616.
40. Rogers, N. K., and Moore, G. R. (1988) On the energetics of conformational changes and pH dependent redox behaviour of electron transfer proteins, *FEBS Lett.* **228**, 69–73.
41. Kannt, A., Lancaster, C. R. D., and Michel, H. (1998) The coupling of electron transfer and proton translocation: electrostatic calculations on *Paracoccus denitrificans* cytochrome *c* oxidase, *Biophys. J.* **74**, 708–721.
42. Popovic, D. M., and Stuchebrukhov, A. A. (2004) Electrostatic study of the proton pumping mechanism in bovine heart cytochrome *c* oxidase, *J. Am. Chem. Soc.* **126**, 1858–1871.
43. Song, Y., Michonova-Alexova, E., and Gunner, M. R. (2006) Calculated proton uptake on anaerobic reduction of cytochrome *c* oxidase: Is the reaction electroneutral?, *Biochemistry* **45**, XXXX–XXXX.
44. Siegbahn, P. E. (2003) The catalytic cycle of tyrosinase: peroxide attack on the phenolate ring followed by O–O cleavage, *J. Biol. Inorg. Chem.* **8**, 567–576.
45. Green, M. T. (1998) Role of the axial ligand in determining the spin state of resting cytochrome P450, *J. Am. Chem. Soc.* **120**, 10772–10773.
46. Guallar, V., and Friesner, R. A. (2004) Cytochrome P450CAM enzymatic catalysis cycle: a quantum mechanics/molecular mechanics study, *J. Am. Chem. Soc.* **126**, 8501–8508.
47. Schoneboom, J. C., and Thiel, W. (2004) The resting state of P450<sub>cam</sub>: A QM/MM study, *J. Phys. Chem. B* **108**, 7468–7478.
48. Ogliaro, F., Harris, N., Cohen, S., Filatov, M., deVisser, D. P., and Shaik, S. (2000) A model “rebound” mechanism of hydroxylation by cytochrome P450: Stepwise and effectively concerted pathways and their reactivity patterns, *J. Am. Chem. Soc.* **122**, 8977–8989.
49. Kamachi, T., and Yoshizawa, K. (2003) A theoretical study on the mechanism of camphor hydroxylation by compound I of cytochrome P450, *J. Am. Chem. Soc.* **125**, 4652–4661.
50. Guallar, V., Baik, M. H., Lippard, S. J., and Friesner, R. A. (2003) Peripheral heme substituents control the hydrogen-atom abstraction chemistry in cytochromes P450, *Proc. Natl. Acad. Sci. U.S.A.* **100**, 6998–7002.
51. Schoneboom, J. C., Cohen, S., Lin, H., Shaik, S., and Thiel, W. (2004) Quantum mechanical/molecular mechanical investigation of the mechanism of C–H hydroxylation of camphor by cytochrome P450<sub>cam</sub>: theory supports a two-state rebound mechanism, *J. Am. Chem. Soc.* **126**, 4017–4034.
52. Brunori, M., Amiconi, G., Antonin, E., Wyman, J., Zito, R., and Fanelli, A. R. (1968) The transition between “acid” and “alkaline” ferric heme proteins, *Biochim. Biophys. Acta* **154**, 315–322.
53. Branden, M., Namslauer, A., Hansson, O., Aasa, R., and Brzezinski, P. (2003) Water-hydroxide exchange reactions at the catalytic site of heme-copper oxidases, *Biochemistry* **42**, 13178–13184.
54. Berman, H. M., Westbrook, J., Feng, Z., Gilliland, G., Bhat, T. N., Weissig, H., Shindyalov, I. N., and Bourne, P. E. (2000) The protein data bank, *Nucleic Acids Res.* **28**, 235–242.
55. Alexov, E. G., and Gunner, M. R. (1997) Incorporating protein conformational flexibility into the calculation of pH-dependent protein properties, *Biophys. J.* **72**, 2075–2093.
56. Georgescu, R. E., Alexov, E. G., and Gunner, M. R. (2002) Combining conformational flexibility and continuum electrostatics for calculating pK<sub>as</sub> in proteins, *Biophys. J.* **83**, 1731–1748.
57. Gunner, M. R., Mao, J., Song, Y., and Kim, J. (2006) Factors influencing energetics of electron and proton transfers in proteins. What can be learned from calculations, *Biochim. Biophys. Acta* (in press).
58. Nicholls, A., and Honig, B. (1991) A rapid finite difference algorithm utilizing successive over-relaxation to solve the Poisson–Boltzmann equation, *J. Comput. Chem.* **12**, 435–445.
59. Bharadwaj, R., Windemuth, A., Sridharan, S., Honig, B., and Nicholls, A. (1995) The fast multipole boundary element method for molecular electrostatics: An optimal approach for large systems, *J. Comput. Chem.* **16**, 898–913.
60. Rocchia, W., Alexov, E., and Honig, B. (2001) Extending the applicability of the nonlinear Poisson–Boltzmann equation: multiple dielectric constants and multivalent ions, *J. Phys. Chem. B* **105**, 6507–6514.
61. Gilson, M. K., and Honig, B. (1988) Calculation of the total electrostatic energy of a macromolecular system: solvation energies, binding energies, and conformational analysis, *Proteins: Struct., Funct., Genet.* **4**, 7–18.
62. Sitkoff, D., Sharp, K. A., and Honig, B. (1994) Accurate calculation of hydration free energies using macroscopic solvent models, *J. Phys. Chem.* **98**, 1978–1988.
63. Song, Y., Mao, J., and Gunner, M. R. (2003) Calculation of proton transfers in bacteriorhodopsin bR and M intermediates, *Biochemistry* **42**, 9875–9888.
64. Cornell, W. D., Cieplak, P., Bayly, C. I., Gould, I. R., Merz, J., K. M., Ferguson, D. M., Spellman, D. C., Fox, T., Caldwell, J. W., and Kollman, P. A. (1995) A second generation force field for the simulation of proteins, nucleic acids, and organic molecules, *J. Am. Chem. Soc.* **117**, 5179–5197.
65. Mao, J., Song, Y., and Gunner, M. R. (2006) Better rotamer packing for continuum electrostatics pK<sub>a</sub> calculations: MCCE2, *J. Comput. Chem.* (in preparation).
66. Becke, A. D. (1993) Density-Functional Thermochemistry. 3. The role of exact exchange, *J. Chem. Phys.* **98**, 5648–5652.
67. Frisch, M. J., Trucks, G. W., Schlegel, H. B., Scuseria, G. E., Robb, M. A., Cheeseman, J. R., Zakrzewski, V. G., J. A. Montgomery, J., Stratmann, R. E., Burant, J. C., Dapprich, S., Millam, J. M., Daniels, A. D., Kudin, K. N., Strain, M. C., Farkas, O., Tomasi, J., Barone, V., Cossi, M., Cammi, R., Mennucci, B., Pomelli, C., Adamo, C., Clifford, S., Ochterski, J., Petersson, G. A., Ayala, P. Y., Cui, Q., Morokuma, K., Malick, D. K., Rabuck, A. D., Raghavachari, K., Foresman, J. B., Cioslowski, J., Ortiz, J. V., Baboul, A. G., Stefanov, B. B., Liu, G., Liashenko, A., Piskorz, P., Komaromi, I., Gomperts, R., Martin, R. L., Fox, D. J., Keith, T., Al-Laham, M. A., Peng, C. Y., Nanayakkara, A., Challacombe, M., Gill, P. M. W., Johnson, B., Chen, W., Wong, M. W., Andres, J. L., Gonzalez, C., Head-Gordon, M., Replogle, E. S., and Pople, J. A. (1998) Gaussian 98, Revision A.9, Gaussian, Inc., Pittsburgh, PA.
68. Richarz, R., and Wüthrich, K. (1975) Carbon-13 NMR chemical shifts of the common amino acid residues measured in aqueous solutions of the linear tetrapeptides H-Gly-Gly-X-L-Ala-OH, *Biopolymers* **17**, 2133–2141.
69. Matthew, J. B., Gurd, F. R. N., Garcia-Moreno, B., Flanagan, M. A., March, K. L., and Shire, S. J. (1985) pH-dependent processes in proteins, *CRC Crit. Rev. Biochem.* **18**, 91–197.
70. Munro, O. Q., and Marques, H. M. (1996) Heme-peptide models for hemoproteins. 1. solution chemistry of *N*-acetylmicroperoxidase-8, *Inorg. Chem.* **35**, 3752–3767.
71. Vashi, P. R., and Marques, H. M. (2004) The coordination of imidazole and substituted pyridines by the hemeoctapeptide *N*-acetyl-ferromicroperoxidase-8 (Fe<sup>II</sup>NACMP8), *J. Inorg. Biochem.* **98**, 1471–1482.
72. Marques, H. M., Cukrowski, I., and Vashi, P. R. (2000) Coordination of weak field ligands by *N*-acetylmicroperoxidase-8 (NACMP8), a ferric haempeptide from cytochrome *c*, and the influence of the axial ligand on the reduction potential of complexes of NACMP8, *J. Chem. Soc.* **2000**, 1335–1342.
73. Santucci, R., Reinhard, H., and Brunori, M. (1988) Direct electrochemistry of the undapeptide from cytochrome *c* (microperoxidase) at a glassy carbon electrode, *J. Am. Chem. Soc.* **110**, 8536–8537.
74. Vanderkooi, G., and Stotz, E. (1965) Reductive alteration of heme a hemochromes, *J. Biol. Chem.* **240**, 3418–3424.
75. Vanderkooi, G., and Stotz, E. (1966) Oxidation–reduction potentials of heme a hemochromes, *J. Biol. Chem.* **241**, 3316–3323.
76. Beroza, P., Fredkin, D. R., Okamura, M. Y., and Feher, G. (1991) Protonation of interacting residues in a protein by a Monte Carlo method: application to Lysozyme and the photosynthetic reaction center of *Rhodobacter sphaeroides*, *Proc. Natl. Acad. Sci. U.S.A.* **88**, 5804–5808.
77. Zhu, Z., and Gunner, M. R. (2005) Energetics of quinone-dependent electron and proton transfers in *Rhodobacter sphaeroides* photosynthetic reaction centers, *Biochemistry* **44**, 82–96.
78. Hay, P. J., and Wadt, W. R. (1985) Ab initio effective core potentials for molecular calculations. Potentials for the transition metal atoms Sc to Hg, *J. Chem. Phys.* **82**, 270–283.
79. Sitter, A. J., Shiflett, J. R., and Terner, J. (1988) Resonance Raman spectroscopic evidence for heme iron-hydroxide ligation in peroxidase alkaline forms, *J. Biol. Chem.* **263**, 13032–13038.
80. Peisach, J., Blumberg, W. E., Ogawa, S., Rachmilewitz, E. A., and Oltzik, R. (1971) The effects of protein conformation on the heme symmetry in high spin ferric heme proteins as studied by electron paramagnetic resonance, *J. Biol. Chem.* **246**, 3342–3355.
81. Honig, B., and Nicholls, A. (1995) Classical electrostatics in biology and chemistry, *Science* **268**, 1144–1149.

82. Gunner, M. R., Saleh, M. A., Cross, E., ud-Doula, A., and Wise, M. (2000) Backbone dipoles generate positive potentials in all proteins: origins and implications of the effect, *Biophys. J.* 78, 1126–1144.
83. Kraus, D. W., Wittenberg, J. B., Lu, J. F., and Peisach, J. (1990) Hemoglobins of the *Lucina pectinata*/bacteria symbiosis. II. An electron paramagnetic resonance and optical spectral study of the ferric proteins, *J. Biol. Chem.* 265, 16054–16059.
84. Sun, J., Wilks, A., Ortiz de Montellano, P. R., and Loehr, T. M. (1993) Resonance Raman and EPR spectroscopic studies on heme-heme oxygenase complexes, *Biochemistry* 32, 14151–14157.
85. Takahashi, S., Wang, J., Rousseau, D. L., Ishikawa, K., Yoshida, T., Host, J. R., and Ikeda-Saito, M. (1994) Heme-heme oxygenase complex. Structure of the catalytic site and its implication for oxygen activation, *J. Biol. Chem.* 269, 1010–1014.
86. Taylor, J. F. (1981) Measurement of the oxidation-reduction equilibria of hemoglobin and myoglobin, *Methods Enzymol.* 76, 577–582.
87. Kraus, D. W., and Wittenberg, J. B. (1990) Hemoglobins of the *Lucina pectinata*/bacteria symbiosis. I. Molecular properties, kinetics and equilibria of reactions with ligands, *J. Biol. Chem.* 265, 16043–16053.
88. Yamada, H., Makino, R., and Yamazaki, I. (1975) Effects of 2,4-substituents of deuteropheme upon redox potentials of horseradish peroxidases, *Arch. Biochem. Biophys.* 169, 344–353.
89. Harbury, H. A. (1957) Oxidation-reduction potentials of horseradish peroxidase, *J. Biol. Chem.* 225, 1009–1024.

BI052182L